# Conserved and Nonconserved Residues in the Substrate Binding Site of 7,8-Diaminopelargonic Acid Synthase from *Escherichia coli* Are Essential for Catalysis†

Jenny Sandmark,‡ Andrew C. Eliot,§ Kristoffer Famm,§ Gunter Schneider,‡ and Jack F. Kirsch*,§

*Department of Medical Biochemistry and Biophysics, Karolinska Institutet, S-171 77 Stockholm, Sweden, and Department of Chemistry, University of California—Berkeley, Berkeley, California 94720-3206*

*Received October 6, 2003*

ABSTRACT: The vitamin $B_6$-dependent enzyme 7,8-diaminopelargonic acid (DAPA) synthase catalyzes the antepenultimate step in the synthesis of biotin, the transfer of the α-amino group of *S*-adenosyl-L-methionine (SAM) to 7-keto-8-aminopelargonic acid (KAPA) to form DAPA. The Y17F, Y144F, and D147N mutations in the active site were constructed independently. The $k_{max}/K_m^{app}$ values for the half-reaction with DAPA of the Y17F and Y144F mutants are reduced by 1300- and 2900-fold, respectively, compared to the WT enzyme. Crystallographic analyses of these mutants do not show significant changes in the structure of the active site. The kinetic deficiencies, together with a structural model of the enzyme-PLP/DAPA Michaelis complex, point to a role of these two residues in recognition of the DAPA/KAPA substrates and in catalysis. The $k_{max}/K_m^{app}$ values for the half-reaction with SAM are similar to that of the WT enzyme, showing that the two tyrosine residues are not involved in this half-reaction. Mutations of the conserved Arg253 uniquely affect the SAM kinetics, thus establishing this position as part of the SAM binding site. The D147N mutant is catalytically inactive in both half-reactions. The structure of this mutant exhibits significant changes in the active site, indicating that this residue plays an important structural role. Of the four residues examined, only Tyr144 and Arg253 are strictly conserved in the available amino acid sequences of DAPA synthases. This enzyme thus provides an illustrative example that active site residues essential for catalysis are not necessarily conserved, i.e., that during evolution alternative solutions for efficient catalysis by the same enzyme arose. Decarboxylated SAM [*S*-adenosyl-(5′)-3-methylthiopropylamine] reacts nearly as well as SAM and cannot be eliminated as a putative in vivo amino donor.

Biotin is essential to all organisms because of its function as a cofactor in carboxylation reactions. It is synthesized in bacteria, plants, and some fungi, while mammals are dependent on obtaining biotin from the diet or from intestinal bacteria. The absence of the biotin biosynthetic pathway in mammals makes it a possible target for safe antibiotics and herbicides (*1*). The pathway requires four committed enzymes (for recent reviews, see refs *2* and *3*), and detailed studies of these enzymes may aid in the design of novel inhibitors. One such antibiotic already exists. Amiclenomycin, originally isolated from a S*treptomyces* species, inhibits 7,8-diaminopelargonic acid (DAPA)[1] synthase specifically (*4*−*6*).

DAPA synthase is a pyridoxal 5′-phosphate- (PLP-) dependent aminotransferase that catalyzes the second step of the pathway, the conversion of 7-keto-8-aminopelargonic acid (KAPA) to DAPA (Scheme 1; *7*). The reaction is typical of PLP-dependent catalysis seen in other aminotransferases (Scheme 2; *8*). However, the enzyme is unique among them in that *S*-adenosyl-L-methionine (SAM) is the amino group donor. Initial, limited kinetic studies of the enzyme (*9*) were followed recently by a more detailed kinetic analysis of recombinant DAPA synthase from *Escherichia coli* (*10*). The *E. coli* enzyme is a homodimer with a molecular mass of 94 kDa. Each subunit has 429 amino acids. The enzyme belongs to subclass II of the fold type I family of aminotransferases (*11*, *12*).

The three-dimensional structures of the DAPA synthase/KAPA complex (*13*) (Figure 1) and that with amiclenomycin (*14*), respectively, led to the identification of the invariant Arg391 as the residue that interacts with the carboxyl group of the bound ligand. The results of a subsequent mutagenesis study are consistent with a role of Arg391 in recognition of the substrates, DAPA and KAPA (*10*). The three-dimensional structure of the enzyme/KAPA complex also revealed a

† This work was supported by NIH Grant GM35393, the Swedish Science Research Council, and the Foundation for Strategic Research through the Structural Biology Network.

* To whom correspondence should be addressed. Telephone: (510) 642-6368. Fax: (510) 642-6368. E-mail: jfkirsch@uclink.berkeley.edu.

‡ Karolinska Institutet.

§ University of California—Berkeley.

[1] Abbreviations: AMPSO, *N*-(1,1-dimethyl-2-hydroxyethyl)-3-amino-2-hydroxypropanesulfonic acid; DAPA, 7,8-diaminopelargonic acid; dcSAM, *S*-adenosyl-(5′)-3-methylthiopropylamine; HEPES, *N*-(2-hydroxyethyl)piperazine-*N*′-2-ethanesulfonic acid; KAPA, 7-keto-8-aminopelargonic acid; MPD, 2-methyl-2,4-pentanediol; PEG, poly(ethylene glycol); PLP, pyridoxal 5′-phosphate; PMP, pyridoxamine 5′-phosphate; rmsd, root mean square deviation; SAM, *S*-adenosyl-L-methionine; WT, wild type.

10.1021/bi0358059 CCC: $27.50 
Published on Web 01/13/2004

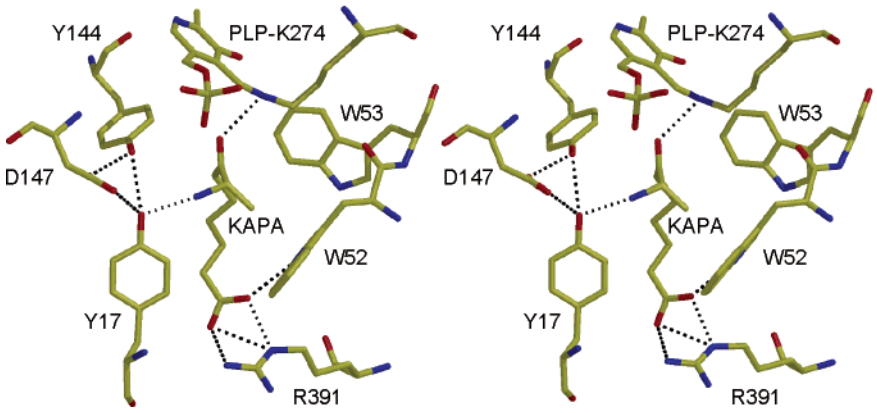


FIGURE 1: Stereoview of the KAPA/DAPA binding site in DAPA synthase as revealed by the three-dimensional structure of the DAPA synthase/PLP/KAPA complex. Hydrogen bonds are represented by dashed lines.

Scheme 1: Reaction Catalyzed by DAPA Synthase

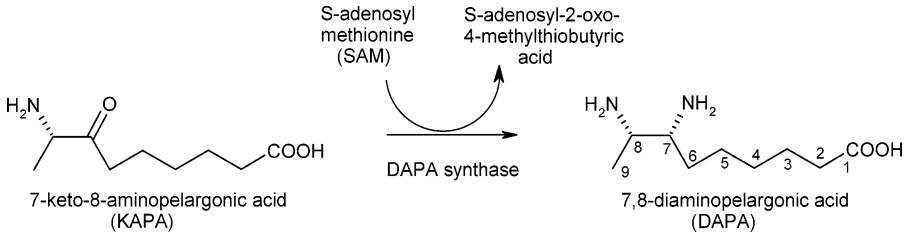


Scheme 2: Aminotransferase Half-Reaction

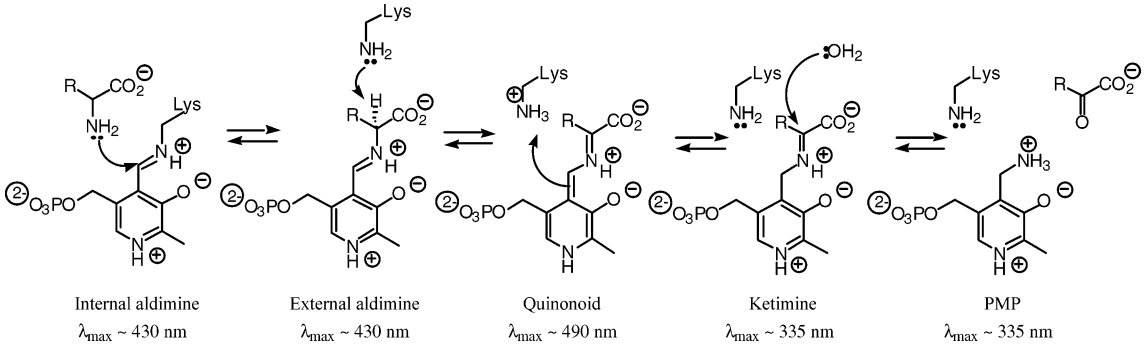


cluster of three residues, Tyr17, Tyr144, and Asp147, in the vicinity of the 8-amino group of the substrate, close to the PLP cofactor. They are connected by a network of hydrogen bonds and appear to be involved in substrate recognition (Figure 1). Tyr17 in particular was predicted to be important, since it is one of the few active site residues that changes conformation upon association with KAPA and it forms a hydrogen bond with the 8-amino group of that substrate. We have now constructed the individual active site mutants Y144F, Y17F, D147N, and R253(A, K, M, Q) to elucidate further the functions of the parent amino acid side chains in the enzymatic mechanism. Specifically, we have studied single-turnover reactions of a selection of these mutant enzymes with the substrates SAM and DAPA, respectively. The three-dimensional structures of the mutant enzymes were determined in order to examine their structural integrity. The results are consistent with a mechanistic proposal in which Tyr17 and Tyr144 participate in recognition of the DAPA/KAPA substrates and in catalysis. They demonstrate further that these residues are not involved in the reaction with the amino donor SAM. Asp147 appears to play a structural role in maintaining the two tyrosine residues in the proper position for catalysis.

## EXPERIMENTAL PROCEDURES

*Reagents.* DAPA was synthesized according to the method of duVigneaud et al. (*15*). dcSAM was kindly provided by Dr. Anthony Pegg (Pennsylvania State University College of Medicine, Hershey, PA). All other reagents are commercially available.

*Mutagenesis, Overexpression, and Purification.* The mutations, Y17F, Y144F, and D147N, were introduced into the *E. coli* DAPA synthase gene with the QuikChange kit (Stratagene). The R253A, R253K, R253Q, and R253M mutations were introduced by standard PCR site-directed mutagenesis protocols. The entire genes were sequenced to ensure that no other mutations were present. The mutant proteins were expressed using the pT7bioA plasmid and purified as described previously (*16*).

*Single-Turnover Reactions of DAPA Synthase with SAM or Decarboxylated SAM.* Mutant DAPA synthase (2.0 $\mu$M) was incubated with varying SAM or decarboxylated SAM (dcSAM; 50−2000 $\mu$M) concentrations in 50 mM AMPSO containing 20% glycerol at pH 9.0. Fluorescence emission ($\lambda_{exc}$ = 330 nm) at wavelengths >360 nm was followed over time with an Applied Photophysics Ltd. SF17.MV spectrof-

Table 1: Data Collection and Refinement Statistics

| | Y17F | Y144F | D147N | R253A | R253K |
|---|---|---|---|---|---|
| unit cell dimensions (Å) | | | | | |
| *a* | 58.5 | 58.8 | 58.4 | 58.3 | 58.1 |
| *b* | 55.7 | 55.3 | 55.1 | 55.7 | 56.5 |
| *c* | 121.4 | 121.5 | 120.3 | 121.2 | 121.0 |
| *β* | 97.0 | 96.8 | 96.7 | 97.0 | 96.3 |
| wavelength (Å) | 1.13 | 1.13 | 1.10 | 0.85 | 1.13 |
| resolution (Å) | 20−1.7 (1.80−1.71)[a] | 20−1.8 (1.93−1.83) | 20−2.1 (2.21−2.10) | 20−2.4 (2.48−2.42) | 20−2.2 (2.32−2.20) |
| $R_{sym}$ (%) | 9.6 (40.8) | 5.2 (21.6) | 8.9 (33.1) | 7.7 (24.8) | 12.4 (42.1) |
| $I/\sigma$ | 11.5 (2.6) | 17.1 (5.2) | 11.8 (2.9) | 14.8 (2.8) | 11.0 (2.4) |
| completeness (%) | 97.2 (90.7) | 99.2 (94.8) | 99.7 (99.2) | 90.6 (55.3) | 99.2 (98.2) |
| no. of reflections | 325020 | 256256 | 149282 | 86216 | 138828 |
| unique reflections | 81351 | 67391 | 44599 | 26936 | 39626 |
| *R* refinement (%) | 18.9 | 18.6 | 20.1 | 18.9 | 19.2 |
| $R_{free}$ (%) | 20.8 | 20.9 | 22.7 | 22.5 | 22.5 |
| *B* factor (Å$^2$) | | | | | |
| Wilson plot | 22.0 | 22.1 | 26.7 | 34.7 | 26.9 |
| protein atoms | 23.2 | 24.9 | 31.9 | 30.8 | 27.6 |
| cofactor | 15.5 | 17.8 | 22.9 | 19.4 | 20.4 |
| water | 35.8 | 34.0 | 32.0 | 35.8 | 31.1 |
| rms deviation | | | | | |
| bonds (Å) | 0.009 | 0.009 | 0.013 | 0.016 | 0.014 |
| angles (deg) | 1.3 | 1.3 | 1.6 | 1.6 | 1.6 |
| Ramachandran plot, % of residues in | | | | | |
| most favorable regions | 89.5 | 89.1 | 90.0 | 89.1 | 88.9 |
| additionally allowed regions | 9.5 | 9.9 | 8.7 | 10.1 | 10.4 |
| generously allowed regions | | | 0.3 | 0.1 | |
| disallowed regions | 1.0 | 1.1 | 1.0 | 0.7 | 0.7 |

[a] Values in parentheses represent the highest resolution shell.

luorometer. Rate constants for the appearance of the product were determined by a nonlinear regression fit to a single exponential. The $k_{max}$ and apparent $K_m$ values for the half-reactions were determined from a plot of the observed rate constants vs substrate concentration according to the formalism outlined in ref *10*.

*Single-Turnover Reaction of DAPA Synthase with DAPA.* Solutions of DAPA synthase mutants (1.0 $\mu$M) in buffer (50 mM AMPSO containing 20% glycerol, pH 9.0) were mixed with DAPA (final concentrations 5, 10, 25, 50, 75 $\mu$M). The fluorescence emission was measured at wavelengths >360 nm with an Applied Photophysics Ltd. SF17.MV stopped-flow spectrofluorometer. The kinetic constants $k_{max}$ and $K_m^{app}$ were determined as described in ref *10*.

*Crystallization and X-ray Data Collection.* The mutant proteins were crystallized by the hanging drop method at 20 °C as described by Käck et al. (*16*). Crystallization was achieved by mixing the well solution (26−28% PEG 4000, 9−12% MPD, 100 mM HEPES, pH 7.5) 1:1 with 10 mg/mL protein. WT crystals were used for microseeding, and crystals appeared within 2 days after the seeding procedure. The R253A data set was collected at beamline BW7B at DESY, Hamburg, with a Marresearch 300 mm image plate, and the data were processed with DENZO (*17*) and SCALEPACK (*18*). All other data sets were collected with a Marresearch CCD detector at beamline I711 at MAX Laboratory, Lund University, Lund, Sweden, at 100 K. The data were processed with MOSFLM (*19*) and SCALA (*18*). The crystals belong to space group $P2_1$ with the dimer in the asymmetric unit, and they diffracted to resolutions ranging from 1.7 to 2.4 Å. Cell dimensions and details of the data collection are given in Table 1.

*Structure Determination.* Structure determination and refinement for each mutant followed the same protocol. The initial phases were obtained from the model of holo-DAPA synthase (*13*) by difference Fourier methods. The initial electron density maps were inspected before replacing the wild-type side chains by the mutated side chain in the model. The structures were refined with Refmac5 (*20*) using the maximum likelihood algorithm. Five percent of the reflections were excluded to monitor $R_{free}$. The O software (*21*) was used for monitoring the refinement progress and manual rebuilding. Water molecules were added to the model and inspected manually during refinement. The quality of the models was assessed with PROCHECK (*22*).

All five mutant structures contain one PLP molecule and one sodium ion per monomer. A number of residues on the surface of the proteins have flexible side chains for which the occupancies were set to 0. Two loop regions in the D147N mutant structure (residues 156−170 and 300−303, respectively) were disordered and were therefore excluded from the model. The final model for this mutant includes residues 1−157, 171−182, 184−299, and 304−429 for monomer A; 1−157, 172−182, 184−298, and 303−428 for monomer B; and 402 water molecules. The final models of the Y17F, Y144F, R253A, and R253K mutants consist of residues 1−182 and 184−428 and include 660, 572, 243, and 336 water molecules, respectively. As a comparison, the final model for the WT structure to 1.8 Å resolution (*13*) contains all residues of the dimer but one (subunit A, 1−182 and 184−429; subunit B, 1−429) and 556 water molecules. Details of the refinement and the stereochemistry of the protein models are given in Table 1. Structural comparisons were carried out using the program O (*21*) with default parameters.

The observed structure factor amplitudes and the refined atomic coordinates have been deposited in the Protein Data Bank with the accession numbers 1S0A (Y17F), 1S09 (Y144F), 1S08 (D147N), 1S07 (R253A), and 1S06 (R253K).

Table 2: Kinetic Parameters for Single-Turnover Half-Reactions of WT and Mutant DAPA Synthases

| | $k_{max}$(SAM) ($s^{-1}$) | $K_m^{app}$(SAM) ($\mu$M) | $k_{max}$(DAPA) ($s^{-1}$) | $K_m^{app}$(DAPA) ($\mu$M) | $k_{max}$(dcSAM) ($s^{-1}$) | $K_m^{app}$(dcSAM) ($\mu$M) |
|---|---|---|---|---|---|---|
| WT | 0.016 (0.004)[a] | 300 (50) | 0.79 (0.01) | 1.0 (0.1) | 0.016 (0.002) | 750 (190) |
| R253A | <0.001 | >1000 | 1.3 (0.05) | 2.2 (0.3) | | |
| R253K | 0.009 (0.001) | 10 (2) | 1.3 (0.09) | 0.8 (0.2) | 0.016 (0.001) | 100 (20) |
| R253Q | 0.074 (0.004) | 105 (14) | 1.7 (0.2) | 1.4 (0.5) | | |
| R253M | <0.01 | | 0.67 (0.05) | 0.6 (0.3) | | |
| Y17F | 0.0035 (0.0006) | 63 (6) | 0.012 (0.001) | 20 (5) | | |
| Y144F | >0.06[b] | >3000[b] | 0.04 (0.002) | 150 (20) | | |
| D147N | nd[c] | nd | nd | nd | | |

[a] Values in parentheses are the calculated errors. [b] The $k_{max}$ and $K_m^{app}$ values could not be determined because this mutant cannot be saturated with SAM. $k_{max}/K_m^{app}$ for this reaction is $16 \pm 1$ $M^{-1}$ $s^{-1}$. [c] No detectable activity.

## RESULTS

The active site residues Tyr17, Tyr144, and Asp147 were replaced by Phe17, Phe144, and Asn147, respectively. The mutant enzymes were analyzed by single-turnover experiments where DAPA or SAM is reacted with the PLP form of the enzyme; thus the two half-reactions may be probed individually. The first is the conversion of SAM to the corresponding keto acid (*S*-adenosyl-4-methylthio-2-oxobutanoate), coupled to the transformation of the PLP form of the enzyme to the pyridoxamine 5′-phosphate (PMP) form (Scheme 2). In the second half-reaction, the PMP form reacts with KAPA to produce DAPA and the PLP enzyme is regenerated. In this study, we analyzed the first half-reaction and the reverse of the second half-reaction, i.e., the reaction of the PLP form of the enzyme with DAPA. The latter was required because the PMP form of DAPA synthase is not stable.

*Kinetic Parameters for the Single-Turnover Transamination of DAPA Synthase Mutants with SAM.* Addition of SAM to the Y17F and Y144F mutants led to the conversion of the 430 nm absorbance peak characteristic for the PLP form of the enzyme to a band at 335 nm, typical for the ketimine or the PMP form of the enzyme. No such spectroscopic change could be detected when the D147N mutant was incubated with 2 mM SAM, indicating that this mutant does not react with this amino donor. The $k_{max}$ and apparent $K_m$ values for the Y17F mutant are 0.0035 $s^{-1}$ and 63 $\mu$M (Table 2), which is a 5-fold decrease in $k_{max}$ and $K_m^{app}$ compared to the WT enzyme with no resulting decrease in $k_{max}/K_m^{app}$. On the other hand, the $k_{max}$ value for the Y144F mutation increases more than 10-fold, but the $K_m^{app}$ value is raised to an unattainable concentration. $k_{max}/K_m^{app}$ is thus reduced more than 3-fold to 16 $M^{-1}$ $s^{-1}$.

*Kinetic Parameters for the Single-Turnover Transamination of DAPA Synthase Mutants with DAPA.* This half-reaction was followed by fluorescence detection ($\lambda_{ex} = 280$ nm) on a stopped-flow spectrophotometer. The D147N mutant reacts with neither DAPA nor SAM (see above); therefore, this form of the enzyme is severely catalytically compromised. The Y17F mutant has an apparent $K_m$ value for DAPA that is 20-fold greater than that for WT and a $k_{max}$ value that is 60-fold lower than that of the WT (Table 2). The Y144F mutation results in a 150-fold increase in apparent $K_m$ for DAPA. The $k_{max}$ is reduced to about 5% of that for the WT reaction.

*The R253A Mutation Increases the $K_m^{app}$ for SAM More Than 10-fold but Has Little Effect on the Reaction with DAPA.* The R253A mutation primarily influences the reaction with SAM. The $k_{max}$ for SAM is reduced to below a measurable level (<0.001 $s^{-1}$), and $K_m^{app}$ is increased to >1 mM (Table 2). The $k_{max}$ and $K_m^{app}$ for DAPA, on the other hand, both *increase*, resulting in a net decrease of $k_{max}/K_m^{app}$ for DAPA of only 25%.

*The Conservative Mutations R253K and R253Q Result in Increases in $k_{max}/K_m^{app}$ for SAM with Little Impact on the Reaction with DAPA.* The more conservative mutations, R253K and R253Q, increase the $k_{max}/K_m^{app}$ for SAM 17-fold and 13-fold, respectively. The increase results from a decreased $K_m^{app}$ for both mutant enzymes and an increase in $k_{max}$ for R253K (Table 2). The R253M mutation was also constructed, but this enzyme is unstable and is nearly inactive.

*Decarboxylated SAM Is Nearly as Reactive as SAM.* Decarboxylated SAM [*S*-adenosyl-(5′)-3-methylthiopropylamine (dcSAM)] was evaluated as a possible alternative substrate with both the WT and R253K mutant enzymes. $k_{max}$ for WT DAPA synthase with this substrate is identical to that obtained with SAM (Table 2), but $K_m^{app}$ is increased 2.5-fold. The R253K mutant enzyme retains the same $k_{max}$ for dcSAM with a decrease in $K_m^{app}$, resulting in a net increase of $k_{max}/K_m^{app}$ of 7.5-fold over WT. This effect, however, is less than the 15-fold increase in $k_{max}/K_m^{app}$ for SAM that results from this mutation.

*Three-Dimensional Structures of DAPA Synthase Mutants.* The crystal structures of the Y17F, Y144F, D147N, R253A, and R253K mutants were refined to 1.7, 1.8, 2.1, 2.4, and 2.2 Å resolution, respectively. The electron density maps are of good quality, and the *R*-factors and stereochemistry are as expected for protein structures at these resolutions (Table 1). The overall folds of the five mutants are identical to the structure of the WT enzyme, as shown by the root mean square deviations calculated for all $C_\alpha$ atoms after superposition with the WT DAPA synthase dimer: 0.13 Å (Y17F), 0.06 Å (Y144F), 0.38 Å (D147N), 0.29 Å (R253K), and 0.30 Å (R253A). The PLP molecule is well-defined in all structures and shows low *B*-factors similar to those of the cofactor in the WT enzyme, indicating high occupancy.

All side chains of the active site residues in the three-dimensional structure of the Y17F mutant occupy the identical position of the corresponding amino acids in the WT enzyme, with the exception of the carboxylate side chain of Asp147, which adopts two roughly equally populated conformations (Figure 2a). One is identical to that of the carboxylate in the structure of the WT enzyme. The other is slightly shifted but is still close enough to Tyr144 to form a hydrogen bond (Figure 2a). There are a number of water molecules at conserved positions in the active site of DAPA

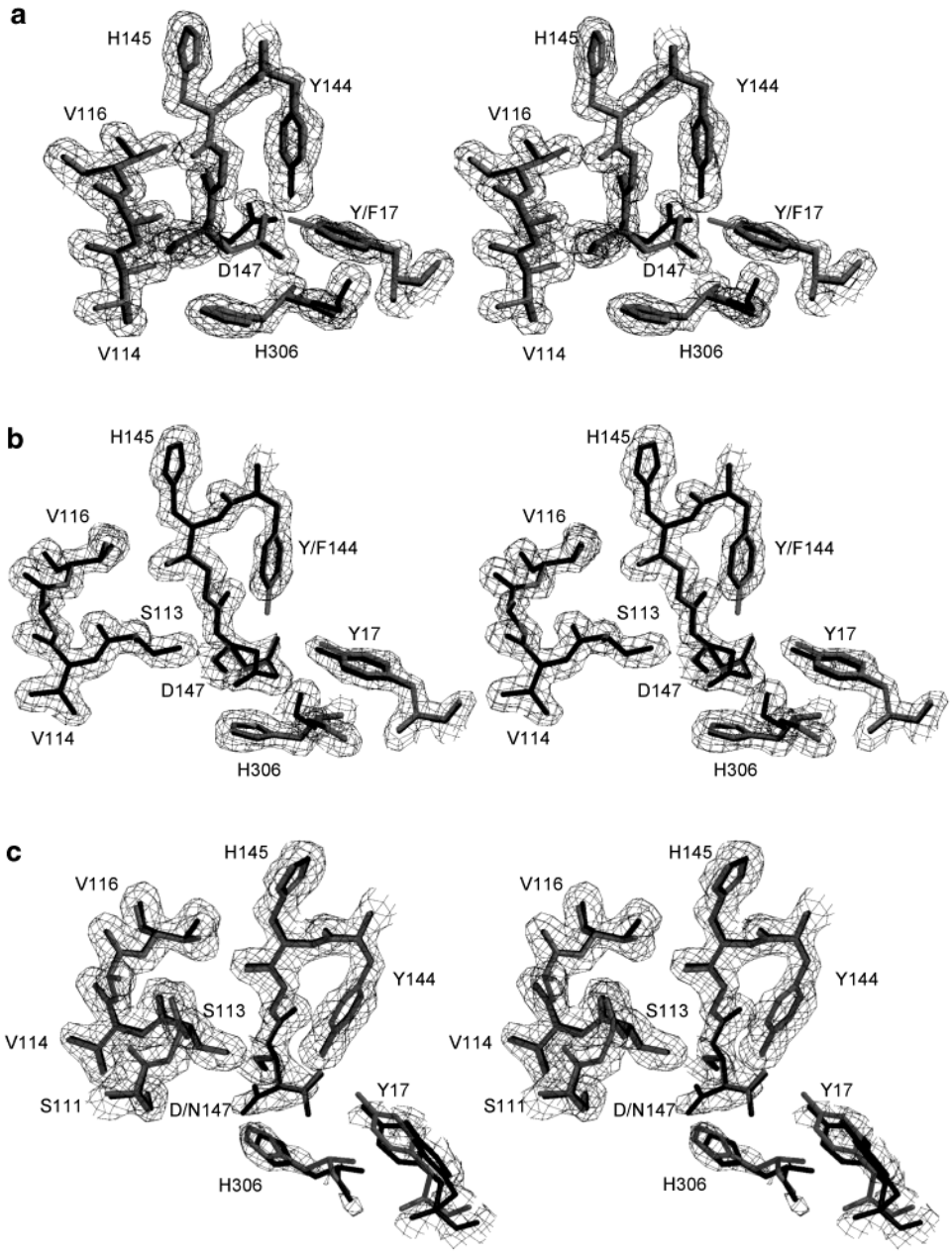


FIGURE 2: Parts of the $2F_o - F_c$ electron density maps for DAPA synthase mutants. The refined model of the mutant is shown in gray and that of WT enzyme in black. Panels: (a) Y17F, contoured at the 1.3$\sigma$ level; (b) Y144F, 1.3$\sigma$; (c) D147N, 1.0$\sigma$.

synthase. The network of solvent molecules around Tyr144 is unperturbed by the mutation, but there is an additional water molecule located halfway between Asp147 and Phe17. This water molecule is within hydrogen-bonding distance of the residues that interact directly with the hydroxyl group of Tyr17 in the WT structure.

The structure of the Y144F mutant is similar to that of the Y17F in that the only difference compared to the WT structure is the double conformation of Asp147. It is a small deviation, and the carboxyl group of Asp147 remains within hydrogen-bonding distance of Tyr17 (Figure 2b). The double conformation does not affect the position or conformation of other residues in the active site. Tyr17 does not deviate from its position in the WT structure, and the side chain of Phe144 superposes very well onto the side chain of the WT Tyr144 (Figure 2b). The water molecules that normally interact with the side chain of Tyr144 are either displaced or missing. There are no water molecules close enough to Phe144 to be able to substitute for the missing hydroxyl group in the structure of the Y144F mutant.

The substitution of Asp147 by an asparagine has, however, more significant consequences for the structural integrity of the active site in DAPA synthase. The side chain of Asn147 is flexible and adopts at least two different rotamer conformations. This movement is more pronounced than for the Y144F and Y17F mutants (Figure 2c). The side chain of Tyr17 is disordered in both subunits and also had to be modeled in two conformations. A stretch of residues, 304−306, close to the active site, carrying the conserved His306, is also disordered in this structure. In addition, the main chain for residues 15−23, including Tyr17, shows a minor shift away from the cofactor.

The R253A mutation induces a significant conformational change in the vicinity of the active site. A stretch of five residues, Ser51−Ala55, is shifted from its original position by several Ångströms, and the main chain adopts a new and

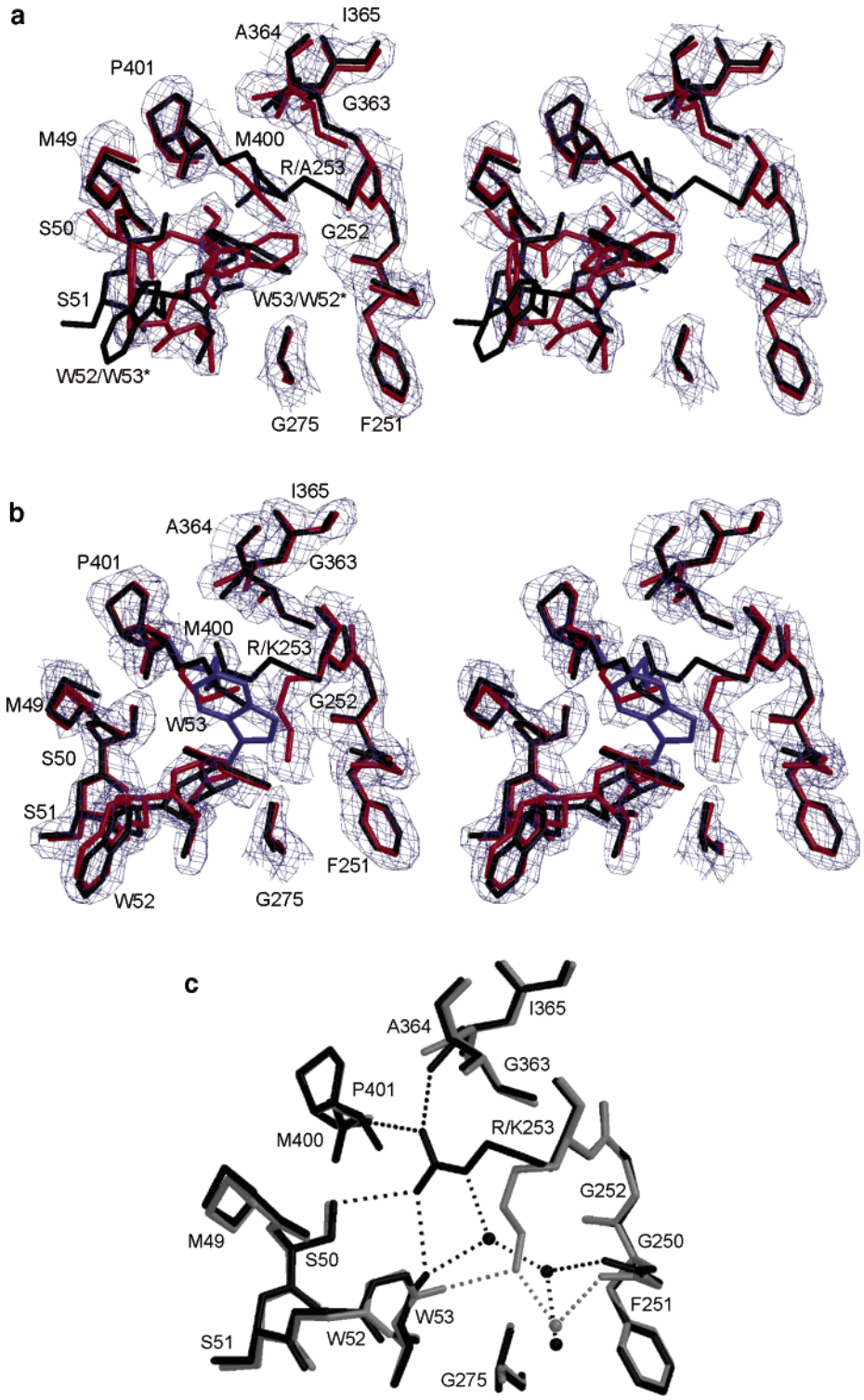


FIGURE 3: (a) Stereoview of the R253A mutant structure (red) superposed onto the structure of the WT DAPA synthase/KAPA complex (black). Residues from R253A are marked with an asterisk where the main chain conformation deviates from WT. The refined $2F_o - F_c$ map is contoured at $1.2\sigma$. (b) Stereoview of the R253K mutant structure (red and blue) superposed onto the WT DAPA synthase/KAPA complex (black). The side chain position of Lys253 differs from WT Arg253. In the mutant structure the side chains of Trp53 and Met400 are modeled in two different conformations (red and blue), one of which (red) corresponds to those observed in the KAPA complex. The second conformation of Met400 (blue) adopts the position occupied by Arg253 in the WT structure, and Trp53 (blue) replaces the side chain of Met400 (red). The refined $2F_o - F_c$ map is contoured at $1.3\sigma$. (c) Superposition of WT DAPA synthase (black) and the structure of the R253K mutant (gray) showing the network of hydrogen bonds involving the side chains of Arg253 and Lys253, respectively. The side chains of Trp52, Trp53, and Met400 are excluded for clarity.

well-defined conformation (Figure 3a). This part of the polypeptide chain includes Trp52 and Trp53, the first of which forms a hydrogen bond to the KAPA carboxyl group in the KAPA complex, and the latter lines the active site. Curiously, even though the main chain is positioned differently, the indole side chains of the two tryptophans are found in positions almost identical to those observed in the WT structure, but they have switched positions; i.e., the side chain

of Trp52 is positioned approximately where the side chain of Trp53 is in the WT structure and vice versa (Figure 3a). The displacement of the main chain as a result of the Arg253 to alanine replacement is probably due to the loss of the hydrogen bond between the guanidinium group of Arg253 and the carbonyl group of Trp53, as well as the displacement of a conserved water molecule that forms hydrogen bonds to both Arg253 and Trp53 (Figure 3c). The interaction between Arg253 and the hydroxyl group of Ser50 is also abolished in the R253A mutant, but this is not likely to be the main cause of the rearrangement of the active site, since this bond is absent in the R253K mutant as well, but it retains the main chain architecture of the active site (see below).

The crystal structure of the R253K mutant showed that, unlike the R253A mutant, the main chain in the active site adopts the position observed in the WT enzyme (Figure 3b). Apparently, the replacement of the arginine residue by lysine does not severely affect the integrity of the active site. The side chain of Lys253 does not superpose onto the Arg253 side chain in the WT structure but forms a hydrogen bond to the main chain carbonyl of Ala248. The side chains of Trp53 and Met400 are modeled in double conformations, one of which corresponds to the positions observed in the structure of the WT enzyme/KAPA complex. In the second conformation, Met400 adopts the position occupied by Arg253 in the WT structures, and the side chain of Trp53 superposes onto the WT conformation of the Met400 side chain (Figure 3b).

*Sequence Conservation.* To further assess the importance of Tyr17, Tyr144, Asp147, and Arg253 in the active site of DAPA synthase, ClustalW (*23*) was used to align 28 microbial amino acid sequences of DAPA synthases that were available in the Swiss-Prot and TrEMBL databases (releases 41.22 and 24.10; Figure 4). The alignment shows that Tyr144 and Arg253 are strictly conserved, while there is always either an aspartic acid or a glutamic acid residue at position 147. Out of the 28 available sequences, 7 contain a glutamic acid at position 147. In these 7 cases, a covariant replacement occurs at position 17, where tyrosine is exchanged for a cysteine residue. Curiously, there are five examples where Tyr17 is replaced by a phenylalanine, but these are not linked to the Asp to Glu replacement at position 147.

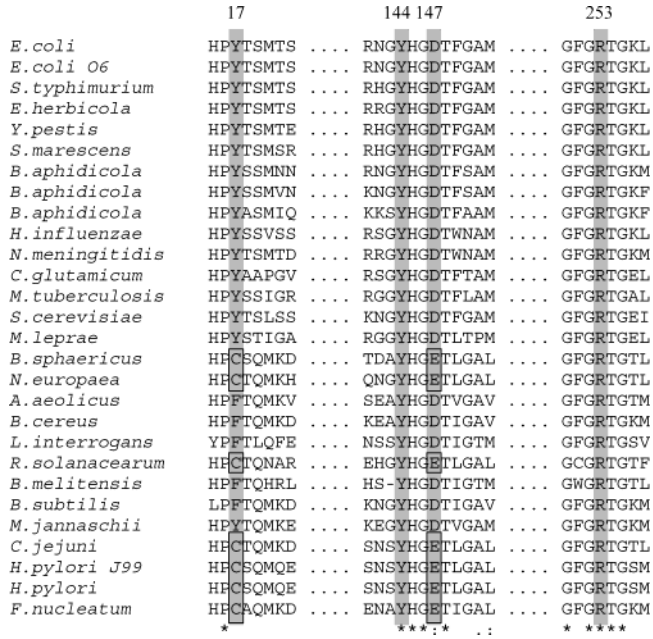


FIGURE 4: Parts of an amino acid sequence alignment of DAPA synthase, highlighting residues Tyr17, Tyr144, Asn147, and Arg253. Seven of the sequences have a cysteine moiety at position 17; the same sequences contain a glutamic acid at position 147. These residues are encircled by black frames. The following DAPA synthase sequences from the Swiss-Prot and TrEMBL databases were aligned with the program ClustalW (*23*), using the slow/accurate pairwise alignment with default options (top to bottom): *Escherichia coli* (P12995), *E. coli* O6 (tr Q8FJQ5), *Salmonella typhimurium* (P12677), *Erwinia herbicola* (P53656), *Yersinia pestis* (tr Q8ZGX3), *Serratia marescens* (P36568), *Buchnera aphidicola ssp. Acyrthosiphon pisum* (P57379), *Buchnera aphidicola ssp. Schizaphis graminum* (Q8K9P0), *Buchnera aphidicola ssp. Baizongia pistaciae* (tr Q89AK4), *Haemophilus influenzae* (P44426), *Neisseria meningitidis* serogroup A (tr Q9JV96), *Corynebacterium glutamicum* (P46395), *Mycobacterium tuberculosis* (O06622), *Saccharomyces cerevisiae* (P50277), *Mycobacterium leprae* (P45488), *Bacillus sphaericus* (P22805), *Nitrosomonas europaea* (tr Q82Y62), *Aquifex aeolicus* (O66557), *Bacillus cereus* strain ATCC 14579/DSM 31 (tr Q818W8), *Leptospira interrogans* (tr Q8F499), *Ralstonia solanacearum* (*Pseudomonas solanacearum*, tr Q8XZC4), *Brucella melitensis* (tr Q8YBV8), *Bacillus subtilis* (P53555), *Metanococcus jannaschii* (Q58696), *Campylobacter jejuni* (tr Q9PIJ2), *Helicobacter pylori* J99 (Q9ZKM5), *Helicobacter pylori* (O25627), and *Fusobacterium nucleatum* (tr Q8RET8). Accession codes are given in parentheses. Sequences obtained from TrEMBL are marked tr above. The sequences are listed according to their alignment score with respect to the *E. coli* sequence, with *S. typhimurium* at the top exhibiting 86% identity and *F. nucleatum* at the bottom showing 30% identity, respectively.

## DISCUSSION

*Tyr17 and Tyr144 Participate in the Half-Reaction with DAPA but Are Not Required for the Reaction with SAM.* The kinetic analysis of site-directed mutants of DAPA synthase from *E. coli* provides compelling evidence that the two tyrosine residues in the KAPA/DAPA substrate binding site are essential for the half-reaction with DAPA but have little influence on the half-reaction with SAM. In both cases, the conservative tyrosine to phenylalanine substitution results in mutant enzymes that are severely impaired in catalytic activity. The $k_{max}/K_m^{app}$ values for the half-reaction with DAPA are reduced 1300-fold for the Y17F mutant and 2900-fold for the Y144F mutant. The crystallographic analysis shows little change in the active site architecture and that interactions within the active site are maintained with the exception of those with the mutated residue. The observed kinetic deficiencies of the mutants are thus not due to structural damage introduced by the mutation but rather reflect a key function of the mutated residue in KAPA/DAPA recognition and catalysis.

The outcome of the Y17F mutation is as anticipated from the structure of the enzyme/KAPA complex. The side chain of this residue binds to the 8-amino group of KAPA and, by inference, that of DAPA (*13*). This interaction might not only provide binding energy and specificity but also appears to be of importance in aligning DAPA in a proper orientation for the reaction to occur (Figure 5). The moderate influence on $K_m^{app}$, if interpreted as affinity for the substrate, may be due to the fact that the 8-amino group forms an additional hydrogen bond to the main chain oxygen of residue 307.

The Y144F mutation results in a dramatic effect on the kinetics of the half-reaction with DAPA, with a 3000-fold

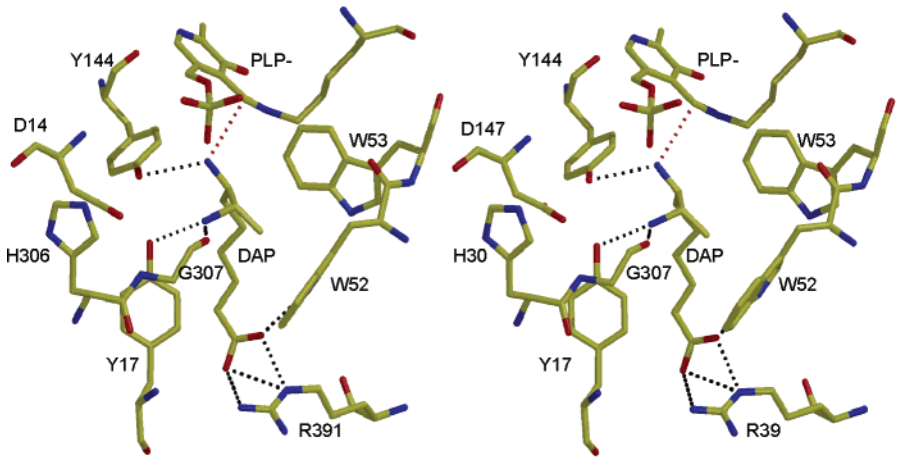


FIGURE 5: Model of the DAPA synthase/DAPA Michaelis complex, which was derived from the crystal structure of the nonproductive DAPA synthase/KAPA complex. All atoms shared by DAPA and KAPA were superposed, and the carbonyl group of KAPA was replaced by the 7-amino group of DAPA with the correct stereochemistry. Hydrogen bonds are shown as dashed lines (black). The distance between the 7-amino group of DAPA and the $C_4'$ of the internal aldimine is approximately 3 Å (red).

decrease in $k_{max}/K_m^{app}$. Tyr144 is thus a key residue in that half-reaction. This conclusion is buttressed by the fact that it is one of the few invariant active site residues in DAPA synthase. Its function can be explained by modeling the DAPA synthase/DAPA Michaelis complex, which is based on the corresponding nonproductive KAPA complex (Figure 5). In this model, which includes the (7*R*,8*S*) DAPA stereochemistry, Tyr144 forms a hydrogen bond to the 7-amino group of DAPA, positioning it so that it is poised for attack on the internal aldimine (3.0 Å distance between the 7-amino group and the $C_4'$ carbon atom of PLP). This residue could thus have several functions: (i) anchoring of the 7-amino group, (ii) ensuring that the proper stereoisomer of the product is obtained, and (iii) maintaining the catalytically competent orientation of the substrate for the transamination reaction. In this orientation, the proton to be abstracted from the C7 carbon of DAPA points toward the putative base in this reaction, Lys274.

Interestingly, both Tyr → Phe mutants show little change in catalytic efficiency for the half-reaction with SAM. The $k_{max}/K_m^{app}$ value for the Y17F mutant is very similar to that for the WT enzyme (56 and 53 $M^{-1}$ $s^{-1}$, respectively), and there is only a 3-fold decrease found for the Y144F mutant, to 16 $M^{-1}$ $s^{-1}$. These observations demonstrate that the two residues have little influence on the reaction of DAPA synthase with the amino donor SAM. The fact that $K_m^{app}$ and $k_{max}$ values vary in parallel for the SAM half-reaction may be indicative of the rate-determining step being product release in the two enzymes. Improved affinity for the substrate would lead to an increase in the affinity for the product, resulting in a decreased reaction rate (in the Y17F mutant) and vice versa for the Y144F mutant.

The mutational analyses suggest that DAPA and SAM bind in nearly completely distinct sites on the enzyme. They both interact with the PLP cofactor and must therefore be bound in its vicinity, but mutation of the residues that are crucial for KAPA/DAPA binding seem not to affect association with SAM. For example, crystallography (*13*) and mutational analyses (*10*) identified Arg391 as one of the key residues in KAPA/DAPA binding, but kinetic characterization of the R391A mutant shows that this residue is not essential for the SAM half-reaction.

*Interactions in the SAM Binding Site.* Although no structure has been solved of a complex with SAM, we postulated on the basis of the structure of the unliganded enzyme that Arg253 might interact with the carboxylate moiety of SAM, as it is the only arginine residue within 15 Å of PLP. It is 12 Å from $C_4'$ of the cofactor but might move closer upon substrate binding, as does Arg386 of AATase (*24*). Arg253 is conserved among all known DAPA synthase sequences (Figure 4), suggesting that it has an important structural or functional role. The R253A, R253K, and R253Q mutations were constructed to investigate this possibility.

*The R253A Mutation Affects Only the Reaction with SAM.* Consistent with the hypothesis, the R253A mutation results in a variant that exhibits a significant increase in the apparent $K_m$ for SAM but has only a small effect on the rate of reaction with DAPA (Table 2). These data strongly support the contention that Arg253 is important for the interaction of the enzyme with SAM but not with DAPA. X-ray analysis, however, revealed that the R253A mutation induces a conformational change of the polypeptide chain near the active site. The effects on the reaction kinetics may, therefore, be the result of this structural change, rather than a direct effect of a lost interaction between the substrate and Arg253.

*The Conservative Mutations R253K and R253Q Increase Activity toward SAM.* The more conservative R253K and R253Q mutant enzymes were constructed to evaluate the role of Arg253 further. The R253K mutant enzyme retains the WT conformation. Both mutations result in a greater than 10-fold *increase* in $k_{max}/K_m^{app}$ for SAM (from 53 $M^{-1}$ $s^{-1}$ for WT to 900 and 700 $M^{-1}$ $s^{-1}$, respectively, for the lysine and glutamine substitutions), with little effect on the DAPA kinetics (Table 2). These results confirm the general conclusions resulting from the R253A mutation results: that the reaction with SAM is affected by changes in this region of the enzyme, while that with DAPA is not. It is therefore established that part of the SAM specificity site does involve Arg253, but the fact that $K_m^{app}$ is *reduced* by these mutations indicates that it does not likely interact directly with the substrate carboxylate (see below).

*Is SAM the True Amino Donor?* Although the 7-amino group of biotin is derived from SAM (*25*, *26*), the high $K_m^{app}$

for SAM and the failure to identify a carboxylate binding site raise the possibility that the in vivo substrate for the enzyme might be the SAM-derived metabolite decarboxylated SAM (dcSAM). This molecule is a precursor to polyamines in most organisms (*27*) and is generated from SAM by decarboxylation (*28*, *29*). Although dcSAM is a substrate for DAPA synthase, with a $k_{max}$ equal to that of SAM, its $K_m^{app}$ value is 2.5-fold higher than that of SAM; thus it is not quite as good a substrate as SAM itself. Since the SAM concentration in the cell is expected to be much higher than that of dcSAM[2] (*30*), it is less likely that dcSAM functions as an in vivo substrate. The comparable $K_m^{app}$ values, however, argue that the carboxylate of SAM is not involved in a strong interaction with the enzyme. DAPA synthase is, therefore, the first known example of an aminotransferase that does not associate with the carboxylate of an α-amino acid substrate via a conserved arginine residue. Further evidence that Arg253 is not responsible for carboxylate binding is provided by the fact that $k_{max}$ for the reaction of the R253K mutant with SAM is unchanged relative to the WT enzyme, but $K_m^{app}$ is reduced (Table 2).

*Asp147 Is Required for Structural Integrity of the Substrate Binding Site.* The D147N substitution, although conservative, results in an enzyme that is devoid of catalytic activity in both half-reactions. This mutation affects the structure in several ways: (i) the side chain shows two rotamers, one of which forms a new set of hydrogen bonds, (ii) Tyr17 is disordered in the structure, (iii) a stretch of residues close to the active site, 304−306, comprising the conserved His306, is disordered, and, finally, (iv) the polypeptide chain of residues 15−23 is slightly shifted from its position in the WT structure. These observations combine to demonstrate that the loss of catalytic activity is primarily due to a structural effect.

*Key Residues in the Active Site of DAPA Are Not Conserved.* Recognition of the substrates DAPA and KAPA is realized by a set of conserved and nonconserved residues in *E. coli* DAPA synthase. In particular, binding of the amino group of the substrate and maintenance of this part of the molecule in a catalytically favorable orientation in the active site are ensured by residues Tyr17 and Tyr144, which are linked via an intricate network of hydrogen bonds that includes Asp147.

Tyr144 is invariant in the 28 available amino acid sequences of DAPA synthase, reflecting its key function in binding the 7-amino group of DAPA. The other two residues, Tyr17 and Asp147, are, however, not strictly conserved. In several sequences, a glutamic acid residue replaces Asp147 with covariant substitution of Tyr17 with a cysteine residue. Modeling of the two residue substitutions suggests that the hydrogen bond between Tyr144 and the carboxyl group of residue 147 can be maintained. Furthermore, the glutamic acid side chain extends far enough into the substrate binding site to form a hydrogen bond to the amino group of KAPA/DAPA. The conformation of the glutamic acid side chain, required for formation of this hydrogen bond, is, however, only possible if the bulky tyrosine side chain at position 17 is replaced by a shorter amino acid, such as cysteine. Since residues 17 and 147 (*E. coli* numbering) always vary in tandem, it is quite possible that a glutamic acid at position 147 may fill the function of anchoring KAPA, in place of Tyr17.

In five of the naturally occurring DAPA synthase sequences, Tyr17 is replaced by phenylalanine, which corresponds to one of the site-directed mutants of this study. The in vitro replacement led to a catalytically defective enzyme, whereas the naturally occurring enzymes with the same mutation must retain sufficient catalytic activity to maintain growth. The deleterious effect on activity of this side chain replacement, seen in the *E. coli* enzyme, must be accompanied by compensating mutations elsewhere in the species with the Y17F replacement. Indeed, there are a number of amino acid side chain replacements in the vicinity of the DAPA binding site in these sequences. It is, however, not clear which and how these side chain substitutions would compensate for the loss of the hydroxyl group at position 17.

DAPA synthase thus illustrates the point that active site residues that contribute to catalysis are not necessarily conserved, i.e., that several solutions for efficient catalysis by the same enzyme arose during the course of evolution.

[2] Although no value for bacterial cells is available, the dcSAM concentration in rat tissue is 2−4% of the SAM concentration, and the $K_m$'s of dcSAM-utilizing enzymes are near 1 μM (*29*).

## ACKNOWLEDGMENT

We acknowledge access to synchrotron radiation at beamlines I711 at MAX Laboratory, Lund University, Lund, Sweden, and BW7B at DESY, EMBL, Hamburg, Germany. We thank all staff members, in particular Yngve Cerenius, for excellent support at the beam lines.

## REFERENCES

1. Rendina, A. R., Taylor, W. S., Gibson, K. J., Lorimer, G. H., Rayner, D., Lockett, B. A., Kranis, K., Wexler, B., Marcovici-Mizrahi, D., Nudelman, A., Nudelman, A., Marsilii, E., Hongji, C., Wawrzak, Z., Calabrese, J., Huang, W., Jia, J., Schneider, G., Lindqvist, Y., and Yang, G. (1999) *J. Pestic. Sci. 55*, 236−247.
2. Marquet, A., Bui, B. T., and Florentin, D. (2001) *Vitam. Horm. 61*, 51−101.
3. Schneider, G., and Lindqvist, Y. (2001) *FEBS Lett. 495*, 7−11.
4. Okami, Y., Kitahara, T., Hamada, M., Naganawa, H., and Kondo, S. (1974) *J. Antibiot. (Tokyo) 27*, 656−664.
5. Poetsch, M., Zahner, H., Werner, R. G., Kern, A., and Jung, G. (1985) *J. Antibiot. (Tokyo) 38*, 312−320.
6. Kern, A., Kabatek, U., Jung, G., Werner, R. G., Poetsch, M., and Zähner, H. (1985) *Liebigs Ann. Chem. 5*, 877−892.
7. Pai, C. H., and McLaughlin, G. E. (1969) *Can. J. Microbiol. 15*, 809−810.
8. Hayashi, H. (1995) *J. Biochem. (Tokyo) 118*, 463−473.
9. Stoner, G. L., and Eisenberg, M. A. (1975) *J. Biol. Chem. 250*, 4037−4043.
10. Eliot, A. C., Sandmark, J., Schneider, G., and Kirsch, J. F. (2002) *Biochemistry 41*, 12582−12589.
11. Jansonius, J. N. (1998) *Curr. Opin. Struct. Biol. 8*, 759−769.
12. Schneider, G., Käck, H., and Lindqvist, Y. (2000) *Struct. Folding Des. 8*, R1−R6.
13. Käck, H., Sandmark, J., Gibson, K., Schneider, G., and Lindqvist, Y. (1999) *J. Mol. Biol. 291*, 857−876.
14. Sandmark, J., Mann, S., Marquet, A., and Schneider, G. (2002) *J. Biol. Chem. 277*, 43352−43358.
15. du Vigneaud, V., Melville, D. B., Folkers, K., Wolf, D. E., Mozingo, R., Keresztesy, J. C., and Harris, S. A. (1942) *J. Biol. Chem. 146*, 475−485.
16. Käck, H., Gibson, K. J., Gatenby, A. A., Schneider, G., and Lindqvist, Y. (1998) *Acta Crystallogr., D: Biol. Crystallogr. 54*, 1397−1398.

17. Otwinowski, Z. (1993) *Proceedings of the CCP4 Study Weekend* (Sawyer, L., Isaacs, N., and Bailey, S., Eds.) pp 55−62, Daresbury Laboratory, Warrington, U.K.
18. Collaborative Computational Project (1994) *Acta Crystallogr. D50*, 760−763.
19. Leslie, A. (1992) in *Joint CCP4 and ESF-EAMCB Newsletter, Protein Crystallography 26*.
20. Murshudov, G. N., Vagin, A. A., and Dodson, E. J. (1997) *Acta Crystallogr, D: Biol. Crystallogr. 53*, 240−255.
21. Jones, T. A., Zou, J. Y., Cowan, S. W., and Kjeldgaard (1991) *Acta Crystallogr. A47*, 110−119.
22. Laskowski, R. A., McArthur, M. W., Moss, D. S., and Thornton, J. M. (1993) *J. Appl. Crystallogr. 26*, 282−291.
23. Higgins, D., Thompson, J., Gibson, T., Thompson, J. D., Higgins, D. G., and Gibson, T. J. (1994) *Nucleic Acids Res. 22*, 4673−4680.
24. Kirsch, J. F., Eichele, G., Ford, G. C., Vincent, M. G., Jansonius, J. N., Gehring, H., and Christen, P. (1984) *J. Mol. Biol. 174*, 497−525.
25. DeMoll, E., White, R. H., and Shive, W. (1984) *Biochemistry 23*, 558−562.
26. Eisenberg, M. A., and Stoner, G. L. (1971) *J. Bacteriol. 108*, 1135−1140.
27. Pegg, A. E. (1986) *Biochem. J. 234*, 249−262.
28. Tabor, C. W. (1962) *Methods Enzymol. 5*, 756−760.
29. Li, Y. F., Hess, S., Pannell, L. K., White Tabor, C., and Tabor, H. (2001) *Proc. Natl. Acad. Sci. U.S.A. 98*, 10578−10583.
30. Cohen, S. S. (1998) *A Guide to Polyamines*, Oxford University Press, New York.

BI0358059